Multi-grid simulation of pedestrian counter flow with topological interaction*

Ma Jian(马 剑)[a)b)], Song Wei-Guo(宋卫国)[a)†], and Liao Guang-Xuan(廖光煊)[a)]

[a)] *State Key Laboratory of Fire Science, University of Science and Technology of China, Hefei* 230026, *China*

[b)] *College of Traffic and Transportation, Southwest Jiaotong University, Chengdu* 610031, *China*

(Received 22 March 2010; revised manuscript received 23 August 2010)

We investigate the dynamics of pedestrian counter flow by using a multi-grid topological pedestrian counter flow model. In the model, each pedestrian occupies multi- rather than only one grid, and interacts with others in the form of topological interaction, which means that a moving pedestrian interacts with a fixed number of those nearest neighbours coming from the opposite direction to determine his/her own moving direction. Thus the discretization of space and time are much finer, the decision making process of the pedestrian is more reliable, which all together makes the moving behaviour and boundary conditions much more realistic. When compared with field observations, it can be found that the modified model is able to reproduce well fitted pedestrian collective behaviour such as dynamical variation of lane formation, clustering of pedestrians in the same direction, etc. The fundamental diagram produced by the model fits also well with field data in the free flow region. Further analyses indicate that with the increase of the size of pedestrian counter flow system, it becomes harder for the system to transit into a jamming state, while the increase of interaction range does not change the transition point from free flow to jamming flow in the multi-grid topological counter flow model. It is also found that the asymmetry of the injection rate of pedestrians on the boundaries has direct influence on the process of transition from free flow to jamming flow, i.e., a symmetric injection makes it easier for the system to transit into jamming flow.

Keywords: pedestrian dynamics, topological interaction, multi-grid model, lane formation

PACC: 8940, 0550, 0570

1. Introduction

Pedestrian traffic has been studied since the early 1960s.[1,2] Many interesting self-organized pedestrian traffic phenomena have been reported, e.g., self-organized lane formation,[1,3] "faster is slower" which means that during evacuation when all the evacuees want to move as fast as possible however the evacuation process will slow down,[4] etc. These reported phenomena significantly affect pedestrians' safety and comfortable level in walking facilities. To study these effects quantitatively, macroscopic and microscopic measurements are proposed. One of the most important macroscopic measurement representations is the fundamental diagram,[5,6] which describes the flow-density relationship. On the basis of such fundamental diagrams, it is found that with the increase of the pedestrian density, pedestrian flow velocity decreases while pedestrian flow rate first increases up to a maximum value and than decreases. It is recently pointed out that the flow remains non-zero even though the density is about 10 persons per square meter.[7] In such a densely packed situation, pedestrians will experience huge stress and feel very uncomfortable. It is believed that the comfortable level of pedestrians in crowds is directly related to the density and the velocity. For this reason, the concept of level-of-service[6,8] was proposed according to the density and the flow rate to describe the service level of different walking facilities.

Although the macroscopic view can provide an overview of pedestrian flow characteristics, they can hardly explain the fundamental principles governing pedestrian dynamics. For the reason that pedestrians are all separated entities, it may be better to describe them as different individuals rather than as an entirety.[9] Microscopic modeling approaches are then developed by taking pedestrian–pedestrian interaction into consideration. When the pedestrians are treated as Newton-like particles, the inter-

*Project supported by the National Natural Science Foundation of China (Grant No. 50678164), the Program for New Century Excellent Talents in University (Grant No. NCET-08-0518), and the National Science and Technology Pillar Program, China (Grant No. 2006BAK06B00).

†Corresponding author. E-mail: wgsong@ustc.edu.cn

© 2010 Chinese Physical Society and IOP Publishing Ltd

actions among pedestrians are described as attraction and repulsive forces,[10] which are influenced by the metric distance between them. Driven by these forces, pedestrians change their velocities from time to time when coming across different circumstances. Models such as the social force model,[10] centrifugal force model,[11] two-dimensional optimal velocity model[12] can well reproduce most of the interesting pedestrian flow phenomena. In addition, discrete models, such as the cellular automaton models,[13−15] lattice gas model,[16,17] multi-grid models,[18] which take into account the human behaviours including forward drift,[19] preferential right,[20] multi-velocity,[21] subconscious behaviour,[22] next-nearest neighbour interaction,[23] k-nearest-neighbour interaction induced decision making[24] and environmental influence,[25−28] can also realize reliable modeling of pedestrian dynamic. The behaviours of the pedestrian may be regarded as being resulted from interactions among pedestrians who are within a given metric distance. However, it is recently demonstrated that topological interaction,[24,29] which is different from the metric distance-based interaction as assumed in most of the previous models, among pedestrians can also play an important role in the emerging of the self-organized lane formation in pedestrian flow.

On the basis of such findings, to check the fundamental laws governing the pedestrian movement, we propose a multi-grid model for pedestrian counter flow by considering a new interaction form, which is both metric and topological in nature. In the model, each pedestrian occupies multi-grids rather than a single grid, and interacts with no more than a fixed number of pedestrians coming from the opposite direction within a given metric distance. We first compare the model results with field data, and then investigate the effects of system size, interaction range, as well as the asymmetric injection rate on the dynamics of pedestrian counter flow.

2. Multi-grid pedestrian counter-flow model

For the reason that a pedestrian will be sensitive only to what happens within a range of a 180° field angle in front of him or her,[30,31,35] we propose a non-isotropic model, named multi-grid topological counter-flow model to investigate pedestrian dynamics. In this model, each pedestrian occupies more than one grids as assumed in Ref. [18]. The effects of both metric distance and topological interaction[24] are taking into account in this model, i.e., the moving features of a pedestrian, taking pedestrian a in Fig. 1 as an example, is determined by the interaction with a fixed number of nearest pedestrians who are in the opposite direction moving to pedestrian a in a given metric distance M. As a result, when only two nearest neighbours are considered, we can see that pedestrians b and d are the nearest neighbours of pedestrian a, and only pedestrian b is in a given metric distance of M from pedestrian a, as a result, moving features of pedestrian a will be influenced by pedestrian b.

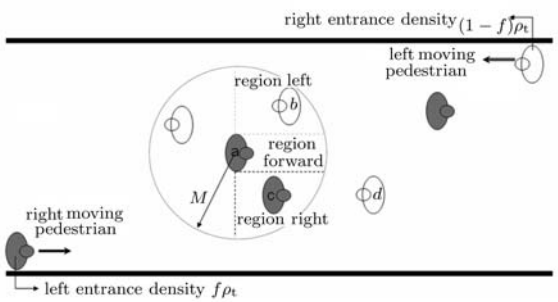


Fig. 1. Interaction pattern of the multi-grid topological counter-flow model.

We construct the multi-grid pedestrian counter flow model on a square lattice channel of $W * L$ cells, where W represents the number of cells in width and L represents the number of cells in length. Each pedestrian can occupy $P * P$ cells. It is assigned that the pedestrians will enter the channel from the left and the right boundaries with a total entrance density of $\rho_{\rm t}$ and will leave the channel from the right and the left boundaries. We further assume the fraction of pedestrians entering from the left boundary, amounting to the total number of pedestrians entering the channel at each time step to be f. After the pedestrians are added into the system at each time step, all the pedestrians in the channel are randomly numbered from 1 to N, where N is the total number of pedestrians at that time step. Then these pedestrians are updated sequentially. Each pedestrian's direction chosen behaviour is determined by the following steps.

Step 1 Calculate the basic transition probability p_m according to the basic configuration that a pedestrian might be encountered in the random walker model as shown in Fig. 2;

Step 2 Find the nearest n neighbours from the opposite direction in a given metric distance M;

Step 3 Calculate the final transition probability p_r according to the distribution of these topological

neighbours by

$$p_r = \frac{p_m T_r}{\sum\limits_{r=m} p_m T_r}, \tag{1}$$

$$T_r = \frac{1}{1+S_r}, \tag{2}$$

where T_r means the topological influence of the neighbours in region r on the corresponding direction m, i.e., right, left and forward regions as shown in Fig. 1, on right, left and forward directions as shown in Fig. 2, respectively; S_r represents the configuration of all the distributed n neighbours, i.e., the number of these pedestrians in each of right, left and forward regions. The formula T_r is chosen to avoid the situation when S_r equals zero and when there is no pedestrian in region r, the probability will not be affected. Condition $r = m$ is set to be a sum representing the influence T_r of pedestrians in region r on the corresponding direction m, i.e., region right on direction right, etc.

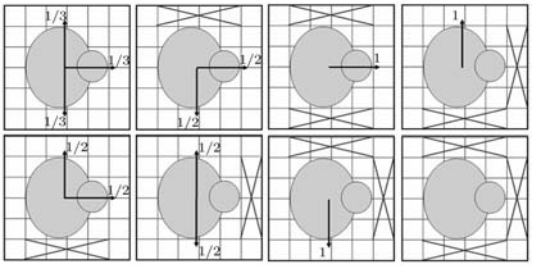


Fig. 2. Possible configurations and the corresponding basic transit probabilities for a right moving pedestrian to be encountered in the random walker model.

3. Comparison with field data

We have carry out simulations on pedestrian counter flow in a channel with $W * L$ cells. The total entrance density $\rho_{\rm t}$ and the fraction of left pedestrians f are kept constant in each simulation. For each simulation, 10000 time steps are taken, and the first 8000 time steps are discarded to let the influence of transit time die out. We first check the lane formation pattern and fundamental diagram of the proposed model. Typical parameters in the simulations performed later are set as follows: $L = 240$, $n = 3$, and $P = 4$.

3.1. Lane formation

To compare the model results with field data, a typical pedestrian crossing scenario is presented in Fig. 3(a). It is easy to find in Fig. 3(a) that when two crowds of pedestrians with different moving directions encounter each other, lanes are formed, which helps the moving people to avoid hitting each other. We also count the number of lanes formed in the scene, with a size of 8 m by 8 m as shown in Fig. 3(a), when the pedestrian density in the region is 0.83–1.28 persons per square meter and the corresponding pedestrian entrance density in these situations is about 0.2–0.5 person/ms in 29 different video recordings. Result is given in Fig. 4(a). We can see that in most of the time, there are formed four or five lanes.

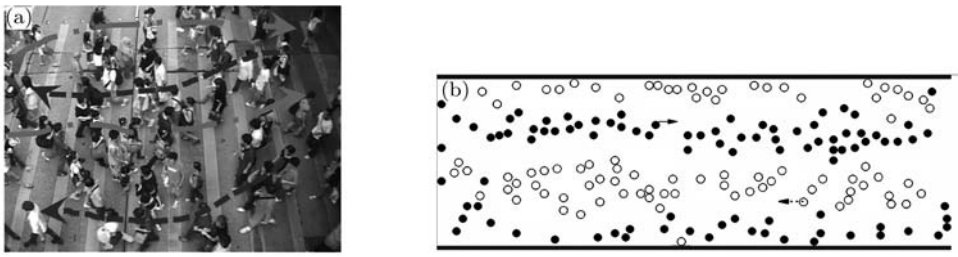


Fig. 3. Comparison of the lane formation pattern between (a) a real pedestrian crossing behaviour and (b) a snapshot of one simulation at the time step of 2500.

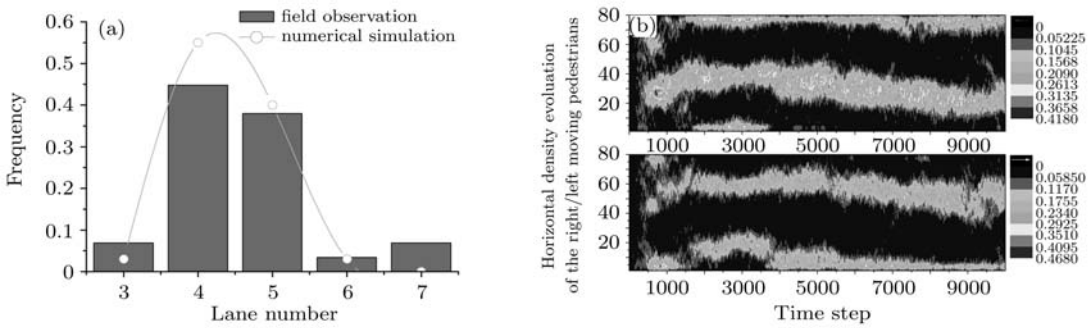


Fig. 4. (a) Frequency distribution of the number of lanes emerging and (b) the density profile evolutions for left-moving and right-moving pedestrians in the multi-grid topological counter flow model.

We then simulate the scenario shown in Fig. 3(a) with $W = 80$ representing the 8-m wide channel. Considering that each pedestrian occupies an area of about 0.4 m by 0.4 m and typical moving velocity of a free moving pedestrian is about 1.45 m/s as indicated in Ref. [33] and about 1.56 m/s with a standard deviation of 0.34 in our field observation, thus, each cell in our model represents an area of 0.1 m by 0.1 m and each time step corresponds to about 0.1 m/(1.56 m/s) = 0.06 s. And for the reason that each pedestrian occupies 4 cells, it takes about 4 time steps for a pedestrian to enter the boundary, we, as a result, set the total entrance density in the model to be 0.16 to represent a pedestrian entrance density of 0.16/(4 time step∗4∗0.4 m∗0.06 s/time step) = 0.42 person/ms. A snapshot of typical pattern formed in one run of the multi-gird topological counter flow model is shown in Fig. 3(b). In a way similar to the case of the real pedestrian traffic, we also find lanes formed in the snapshot of the running process of the model, which is presented in Fig. 3(b). Right moving pedestrians, denoted by the black solid circles, are running one after another, so do the left moving pedestrians. We can also find in Fig. 3(b) that the number of lanes formed in the channel is four at this time step. However, it should also be noted that the lane formation pattern is dynamically varying, or in other words, the number of lanes formed in a given section of the channel is time-dependent but not constant as pointed out by Helbing in Ref. [1]. We then check the evolution of lane formation pattern in the proposed multi-grid topological counter flow model. Density profiles for the left moving pedestrians and the right moving pedestrians at different time steps of the simulation are shown in the upper and lower parts of Fig. 4(b), respectively. In this figure, each pixel value is calculated by $N_{t,y}/L$, where $N_{t,y}$ denotes the number of left (right) moving pedestrians in the line y at the time step t. As we can count, the number of lanes is time-dependent, i.e., mainly changing from 5 at the beginning to 4 lanes after the time step 6000 in the channel. We further count the time steps each number of lanes emerging, and then calculate the corresponding frequency, which is plotted in Fig. 4(a). As we can find, the frequency of the number of lanes emerging fits well to field observations, too.

3.2. Fundamental diagram

In this part, we check the fundamental diagram of the proposed multi-grid topological counter flow model, and compare it with empirical results obtained by Weidmann,[34] Older[35] for the bi-directional flow under open boundary condition. Flow rate here is calculated by counting the number of pedestrians left from the boundaries at each time step of the simulation. The corresponding number of pedestrians in the channel is also counted. We then plot the fundamental diagram in Fig. 5. It should be noticed that the results are averaged results of 10 different runs. From Fig. 5 we can find that the model can also well capture the flow-density relation in the free flow region, but cannot well capture the characteristic of the congestion region. This is because in dense crowd the space might occupy smaller space than 0.16 m^2, which has been built in the model.

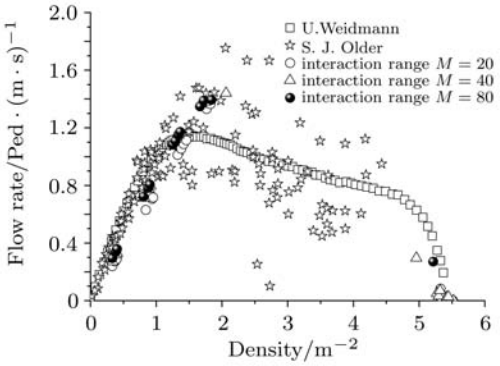


Fig. 5. Comparison of fundamental diagram between multi-grid topological counter flow model and empirical results.

4. Simulation and discussion

We further investigate the effect of system size on the relation between mean velocity and total entrance density, and finally study the relations between mean velocity and total entrance density and between occupancy of pedestrians and the total entrance density. Mean velocity in this paper is defined as the number of walkers moving forward divided by the total number of walkers in the channel. Occupancy is defined as the total number of walkers in the channel, divided by the maximum number of walkers the channel can hold, i.e., $N * P * P/(W * L)$.

4.1. Effect of system size

We check the effects of system size on the movement of pedestrians in counter flow. Figure 6 shows the plots of mean velocity against total entrance density for different channel widths, i.e., $W = 40$, 80, 120, 160 and 240, and the plots of the critical total

entrance density against the inverse of W, i.e., $1/W$. From Fig. 6(a) we can see that the trends of the curves are almost the same, which means the mean velocity of pedestrians will be barely influenced by the channel width. However, the transitions from free flow to jamming flow become sharper with channel width increasing. Owing to the fact that the transitions occur at almost the same values for different channel widths as reflected by Fig. 6(b) and for the sake of computing, we choose $W = 40$ in the following simulations.

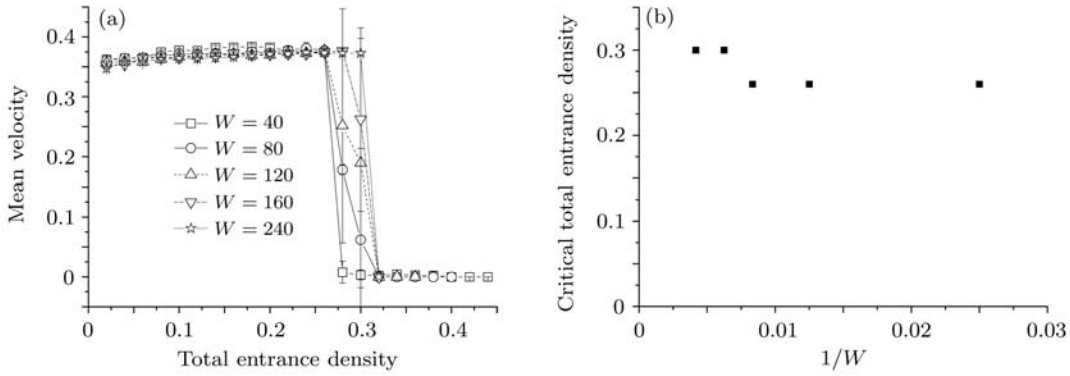


Fig. 6. (a) Effects of system size on the relation between mean velocity and total entrance density and (b) plots of the critical total entrance density against the inverse of W, $1/W$ with $L = 240$, $M = 20$, $f = 0.5$ and $n = 3$.

4.2. Effect of range of interaction

As mentioned above in the model description section, the interaction in the proposed multi-grid model is some kind of long range interaction rather than immediate interaction in traditional models. However, confined by factors such as view field, pedestrians cannot interact with those who are too far away. So, we check the effect of interaction range here in this subsection on the mean velocity as well as on the occupancy of the channel.

The simulation results of the model are presented in Fig. 7. Interaction ranges in these models are set to be $M = 20$, 40 and 80 cells, i.e., about 2 m, 4 m and 8 m, when the fraction of pedestrians entering from the left boundary is $f = 0.5$. The result for a random walker model, i.e. without topology interaction, is

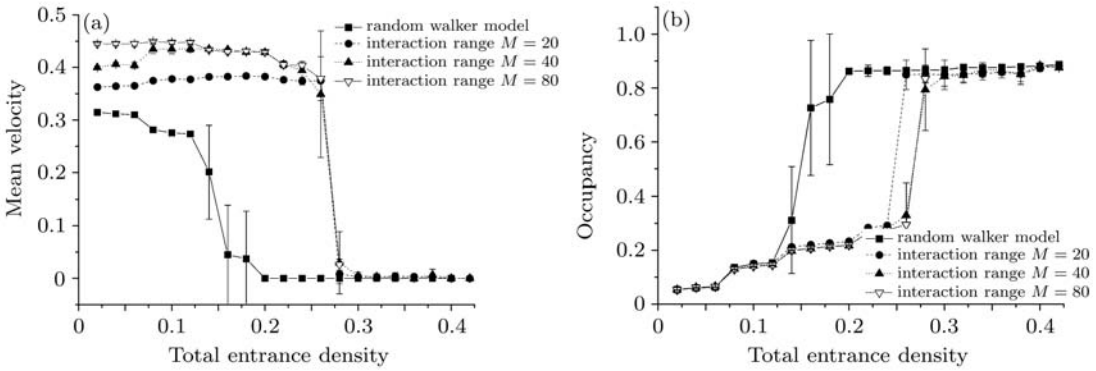


Fig. 7. Effects of interaction range on relations (a) between mean velocity and total entrance density and (b) between occupancy and total entrance density when the fraction of pedestrians entering from the left boundary is 0.5.

also presented for comparison. As shown in Fig. 7, with the increase of the total entrance density, pedestrian mean velocity in the random walker model always decreases, while in the multi-grid model with long range topological interaction it first increases and then decreases, and finally all remain at a value of zero, implying that a phase transition from free flow to jamming flow occurs. When referring to the occupancy of the channel, we find with the increase of the total entrance density, the occupancy increases no matter whether the long range interaction is considered. We can also find in Fig. 7(a) that when the

interaction range increases from 2 m to 4 m, mean velocity of the pedestrians in the free flow region increases, and when the interaction range increases from 4 m to 8 m, the mean velocity increases only in the low total entrance density region, there is not much difference between the mean velocity of pedestrians with an interaction range of 4 m and the mean velocity of pedestrians with an interaction range of 8 m when the total entrance density comes across 0.14. It should also be noticed that with the consideration of the topological interaction, the transition from free flow to jamming flow occurs at a much higher value as compared with that of the model when topology interaction is not taken into account. However, the interaction range itself does not change the transition point for the multi-grid models with topological interaction. The same results could also be obtained from the curve for occupancy vs. total entrance density relation as shown in Fig. 7(b). Compared with the mean velocity differences for different interaction ranges, the occupancy difference is not so significant.

4.3. Effect of asymmetric injection rate

We study the flow patterns when the number of pedestrians entering from the left and the right boundaries are not the same. This asymmetric injection process is realized by changing the fraction of left moving pedestrians among the total number of pedestrians entering into the system at each time step. In Fig. 8, typical mean velocity patterns for the random walker model and the multi-grid topological counter flow model are presented. From these figures we can find almost the same characteristics as those shown in Fig. 7. The mean velocity of pedestrians for the random walker model is plotted in Fig. 8(a). From this figure we can see that when the total entrance density is small, the mean velocities are almost the same for different values of f. With the increase of the total entrance density, the difference becomes obvious. The flow for the symmetry entrance density, i.e., the case of $f = 0.5$, transits into jamming pattern first, while the most asymmetric flow, i.e., the case when $f = 0.1$, transits from free flow into jamming pattern finally. In other words, with the decrease of f, the flow pattern becomes more and more stable. This is because jam formation is triggered by slight cluster formation as shown in Fig. 9. A higher asymmetric injection rate of pedestrians makes the cluster formation harder, which further leads to the occurrence of the transition from free flow to jamming flow at a much higher total entrance density.

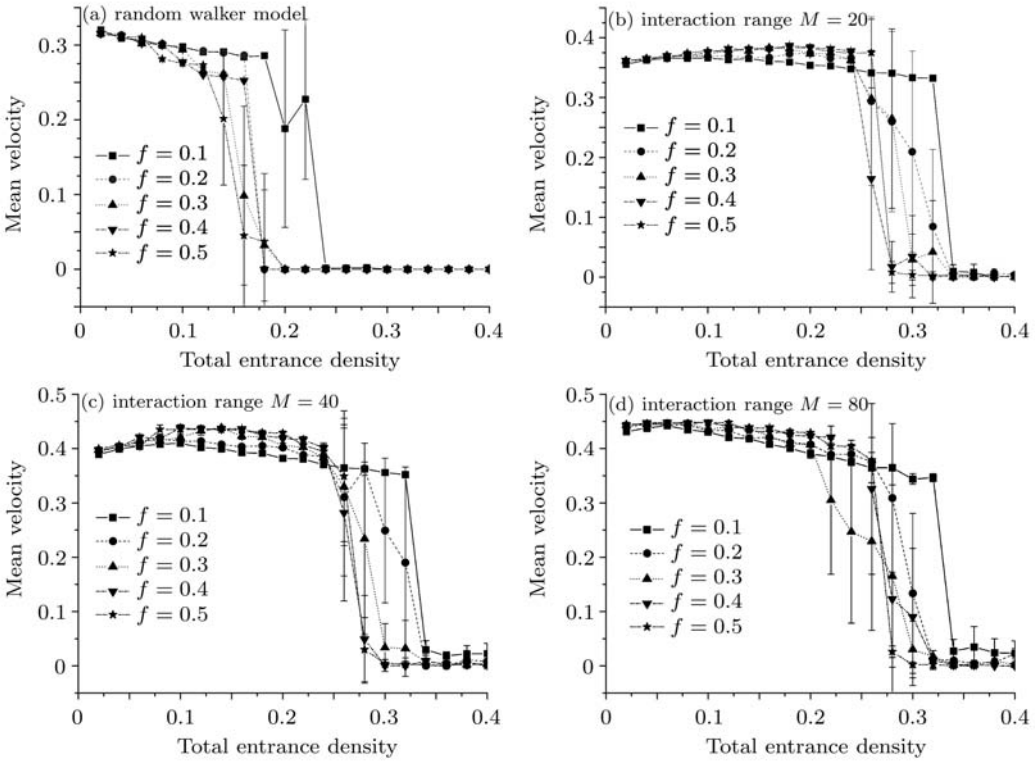


Fig. 8. Effects of asymmetric interaction rate on relations between the mean velocity and total entrance density for the random walker model (a) and for the multi-grid model with an interaction range of $M = 20$ (b), 40 (c) and 80 (d).

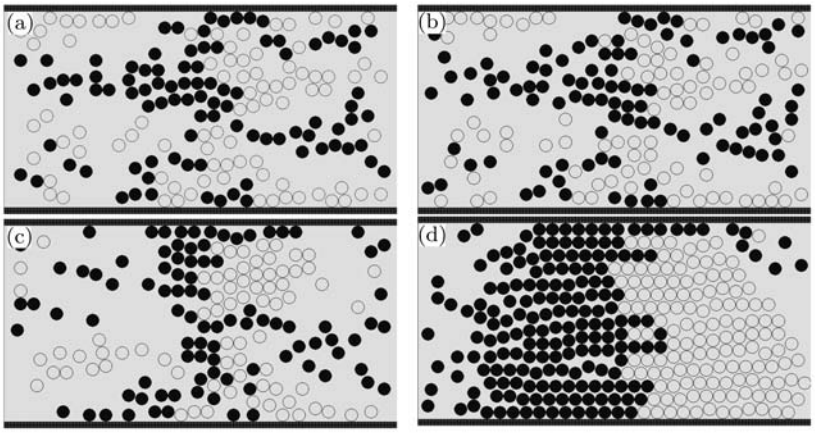


Fig. 9. Typical patterns of jam formation at different time steps of the simulation.

In Figs. 8(b)–8(d), we can find the mean velocity against total entrance density for the case where different interaction ranges are considered. As we can see in these figures, the mean velocity of pedestrian first increases, then decreases and finally reaches zero with the increase of the total entrance density, which indicates that a phase transition from free flow to jamming flow also occurs when the topological interaction is considered. With the increase of f, the difference among velocities increases with the increase of total entrance. A small f makes a high value of transition point from free flow to jamming flow. However, when we fix f, and then check the transition points for different interaction ranges, we find that for a fixed value of f, the transition from free flow to jamming flow occurs at the same total entrance density, no matter what the value of interaction range is. The effect of interaction range is that with a larger interaction range, more information about the real time traffic configurations can be obtained by the object pedestrians, which then makes the direction chosen behaviour much more effective in promoting the efficiency of the pedestrian dynamics.

Typical relations between occupancy and total entrance density for the random walker model and the multi-grid topological counter flow are plotted in Fig. 10. In Fig. 10(a), the occupancy of pedestrians in the

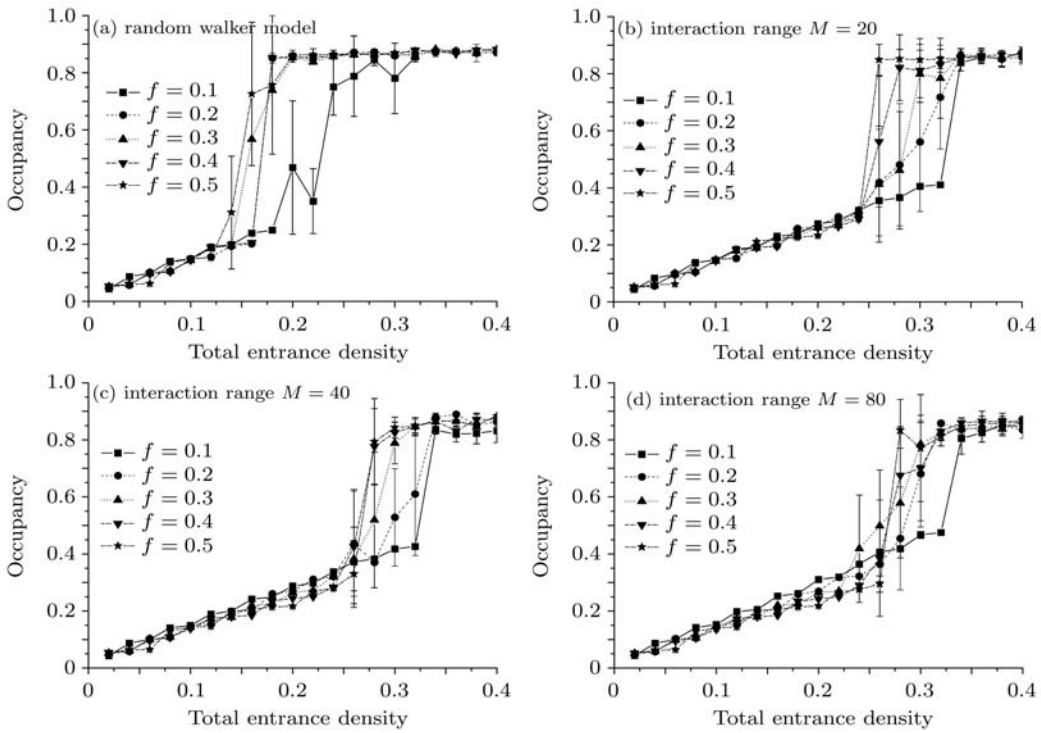


Fig. 10. Effects of asymmetric interaction rate on the occupancy for random walker model (a) and for multi-grid model with an interaction range of $M = 20$ (b), 40 (c) and 80 (d).

channel for the case where there is no topological interaction is plotted. From the figures we can see that with the increase of the total entrance density, the occupancies increase for all fractions of right moving pedestrians. From the analysis detailed above, we find similar characteristics in the trend of the occupancy vs. total entrance density for the multi-grid topological counter flow model.

5. Conclusions

This article presents a study of pedestrian dynamics by establishing a multi-grid topological counter flow model. In the model, pedestrians occupy multi-grids and as a consequence the pedestrians move much reliably as compared with real situations. The interaction in this model is both metric and topological in nature, which means the interaction among the pedestrians is influenced by both the pedestrian–pedestrian metric distance and the topological distance. In other words, one pedestrian interacts with no more than a fixed number of pedestrians coming from the opposite direction within a given distance, the interaction range. Our findings are as follows.

(i) The model can well capture pedestrian counter flow characteristics such as the dynamically varying lane formation, clustering of pedestrians moving in the same moving direction, etc.

(ii) The fundamental diagram of the proposed model fits also well to the empirical results of pedestrian counter flow.

(iii) With the increase of the size of the pedestrian counter flow system, it becomes harder for the system to transit into jamming state.

(iv) The interaction range itself does not change the transition point from free flow to completely jamming flow, however, do enlarge the free flow region as compared with the case where no topological interaction is taken into account. A larger interaction radius will improve the mean velocity of the pedestrians for the reason that more information about the self-organized pedestrian counter flow is provided.

(v) The asymmetric injection rate of pedestrians from different boundaries affects the transition from free flow to jamming flow. An asymmetric injection rate leads to a much stable counter flow, which means most of the pedestrians can move freely when only a few pedestrians come from the opposite, and the transition from free flow to jamming flow can occur only at higher total entrance density as compared with symmetric flow.

References

[1] Helbing D 2001 *Rev. Mod. Phys.* **73** 1067

[2] Helbing D, Buzna L, Johansson A and Werner T 2005 *Transport. Sci.* **39** 1

[3] Helbing D, Johansson A and Lammer S 2008 *The Dynamics of Complex Urban Systems* Monte Verità in Ascona/Ticino, Switzerland, Novermber 2–6, 2004 pp. 287–309

[4] Helbing D, Farkas I and Vicsek T 2000 *Nature* **407** 487

[5] Seyfried A, Bernhard S, Wolfram K and Maik B 2005 *J Stat. Mech. — Theory* E **10** P10002

[6] Fruin J J 1971 *Pedestrians, Highway Research Board* **377** 1

[7] Helbing D, Johansson A and Al-Abideen H Z 2007 *Phys. Rev.* E **75** 046109

[8] Lee J Y S, Goh P K and Lam W H K 2005 *J. Transp. Eng. Asce.* **131** 957

[9] Seyfried A, Steffen B and Lippert T 2006 *Physica* A **368** 232

[10] Helbing D and Molnàr P 1995 *Phys. Rev.* E **51** 4282

[11] Yu W J, Chen R, Dong L Y and Dai S Q 2005 *Phys. Rev.* E **72** 026112

[12] Nakayama A, Hasebe K and Sugiyama Y 2005 *Phys. Rev.* E **71** 036121

[13] Song W G, Yu Y F, Wang B H and Fan W C 2006 *Physica* A **371** 658

[14] Weng W G, Yuan H Y, Fan W C and Hasemi Y J 2007 *Int. J. Mod. Phys.* C **18** 927

[15] Yue H, Shao C F, Chen X M and Hao H R 2008 *Acta Phys. Sin.* **57** 6901 (in Chinese)

[16] Jiang R and Wu Q S 2007 *Physica* A **373** 683

[17] Li X M, Chen T, Pan L L, Shen S F and Yuan H Y 2008 *Physica* A **387** 5457

[18] Song W G, Xu X, Wang B H and Ni S J 2006 *Physica* A **363** 492

[19] Tajima Y, Takimoto K and Nagatani T 2002 *Physica* A **313** 709

[20] Muramatsu M, Irie T and Nagatani T 1999 *Physica* A **267** 487

[21] Zhou J W, Chen X L, Zhou J H, Tan H L, Kong L J and Liu M R 2009 *Acta Phys. Sin.* **58** 2281 (in Chinese)

[22] Kuang H, Song T, Li X L and Dai S Q 2008 *Chin. Phys. Lett.* **25** 1498

[23] Wen J, Tian H H and Xue Y 2010 *Acta Phys. Sin.* **59** 3817 (in Chinese)

[24] Ma J, Song W G, Zhang J, Lo S M and Liao G X 2010 *Physica* A **389** 2101

[25] Tian H, Xue Y and Wei Y F 2009 *Int. J. Mod. Phys.* C **20** 1001

[26] Yu Y F and Song W G 2007 *Phys. Rev.* E **75** 046112

[27] Bing Q, Tan H L, Kong L J and Liu M R 2004 *Chin. Phys.* **13** 990

[28] Guo R Y and Huang H J 2010 *Chin. Phys.* B **19** 030501

[29] Ballerini M, Calbibbo N, Candeleir R, Cavagna A, Cisbani E, Giardina I, Lecomte V, Orlandi A, Parisi G, Procaccini A, Viale M and Zdravkovic V 2008 *P. Nat. Acad. Sci. USA* **105** 1232

[30] Johansson A, Helbing D and Shukla P 2007 *Adv. Complex Syst.* **10** 271

[31] Moussaid M, Helbing D, Garnier S, Johansson A, Combe M and Theraulaz G 2009 *P. Roy. Soc.* B: *Biol. Sci.* **276** 2755

[32] Ma J, Song W G, Fang Z M, Lo S M and Liao G X 2010 *Build. Environ.* **45** 1260

[33] Lam W H K and Cheung C Y 2000 *J. Transp. Eng. Asce.* **126** 343

[34] Weidmann U 1993 *Transporttechnik der Fuβganger* (Vol. 90), (ETH Zürich: Straβen- undEisenbahnbau)

[35] Older S J 1968 *Traffic Eng. Cont.* **10** 160